Volume 13, Issue 4, Page 58-65, 2024 https://doi.org/10.46810/tdfd.1497634 Research Article

BİNGÖL UNIVERSITY

Türk Doğa ve Fen Dergisi
Turkish Journal of Nature and Science
www.dergipark.gov.tr/tdfd

# Investigation of the Catalytic Effect of ZnO Produced by Green Synthesis on $NaBH_4$ Hydrolysis

**Mehmet Erman MERT[1*], Başak DOĞRU MERT[2]**

[1] Adana Alparslan Türkeş Science and Technology University, Advanced Technology Research and Application Center, Adana, Türkiye
[2] Adana Alparslan Türkeş Science and Technology University, Engineering Faculty, Energy Systems Engineering Department, Adana, Türkiye
Mehmet Erman MERT ORCID No: 0000-0002-0114-8707
Başak DOĞRU MERT ORCID No: 0000-0002-2270-9032

**Corresponding author: memert@atu.edu.tr*

(Received: 14.06.2024, Accepted: 26.10.2022, Online Publication: 30.12.2024)

**Keywords**
Green chemistry, Hydrgen generation, $NaBH_4$ hydrolysis, TEM, ZnO

**Abstract:** This study investigates the catalytic performance of ZnO nanoparticles (NPs) synthesized using ethanolic turmeric extract for the hydrolysis of $NaBH_4$. The ZnO NPs were characterized using scanning electron microscopy (SEM), energy dispersive X-ray analysis (EDX), and transmission electron microscopy (TEM) to determine their morphology and elemental composition. Ultraviolet (UV) spectroscopy and zeta potential measurements were also conducted to evaluate optical properties and colloidal stability. The ZnO NPs exhibited granular morphology with an average diameter of 0.6 µm and a Zn-to-O weight ratio of 57:43. Particle size distribution ranged from 30 nm to 70 nm, enhancing catalytic efficiency by increasing the surface area-to-volume ratio and active sites for the hydrolysis reaction. UV spectra revealed absorption peaks at 253 nm, 513 nm, and 977 nm, indicating intrinsic bandgap absorption and surface-related states. The zeta potential of -5.78 mV suggested moderate stability, with some agglomeration observed in solution. The ZnO NPs significantly improved hydrogen generation, increasing the hydrogen volume from 29.4 mL to 383.4 mL, achieving nearly a 13-fold enhancement in $NaBH_4$ hydrolysis.



# Yeşil Sentez ile Üretilen ZnO'nun $NaBH_4$ Hidrolizi Üzerindeki Katalitik Etkisinin İncelenmesi

**Anahtar Kelimeler**
Yeşil kimya, Hidrojen üretimi, $NaBH_4$ hidrolizi, TEM, ZnO

**Öz:** Bu çalışma, $NaBH_4$'ün hidroliz reaksiyonu için etanolik zerdeçal özütü kullanılarak sentezlenen ZnO nanopartiküllerinin (NP'ler) katalitik performansını araştırmaktadır. ZnO NP'lerin morfolojisi ve elementel bileşimini belirlemek amacıyla taramalı elektron mikroskobu (SEM), enerjı dağılımlı X-ışını analizi (EDX) ve transmisyon elektron mikroskobu (TEM) ile karakterizasyon yapılmıştır. Optik özellikleri ve kolloidal kararlılığı değerlendirmek için ultraviyole (UV) spektroskopisi ve zeta potansiyel ölçümleri de gerçekleştirilmiştir. ZnO NP'lerin ortalama 0,6 µm çapında granüler bir morfolojiye ve %57 Zn ile %43 O ağırlık oranına sahip olduğu belirlenmiştir. Parçacık boyutu dağılımının 30 nm ile 70 nm arasında değişmesi, yüzey alanı/hacim oranını ve reaksiyon için aktif alanları artırarak katalitik verimliliği artırmıştır. UV spektrumları, 253 nm, 513 nm ve 977 nm'de doruklar göstermiş ve bu doruklar, içsel bant aralığı soğurması ve yüzeyle ilişkili durumlarla ilişkilendirilmiştir. -5,78 mV olarak ölçülen zeta potansiyeli, çözeltide bir miktar aglomerasyon gözlenmesine rağmen, orta derecede bir kararlılık önermiştir. ZnO NP'ler, $NaBH_4$ hidrolizinde üretilen hidrojen miktarını 29,4 mL'den 383,4 mL'ye çıkararak hidrojen üretiminde yaklaşık 13 katlık bir artış sağlamıştır.

## 1. INTRODUCTION

Hydrogen is a important energy carrier in the global transition towards clean and sustainable energy systems. Its significance arises from its ability to function as both a clean fuel and a key enabler for reducing greenhouse gas emissions, offering practical solutions to the growing demand for sustainable energy alternatives. Due to its role in mitigating environmental challenges, hydrogen has become central to various national and international strategies focused on achieving net-zero emissions. In addition to its environmental benefits, hydrogen plays a significant role in industrial processes, including the synthesis of chemical compounds, petroleum refining, and the production of ammonia for fertilizers [1-3]. An essential application of hydrogen lies in the development of fuel cells, which provide a promising alternative to conventional fossil fuel-based energy sources. Fuel cells convert hydrogen into electricity with high efficiency, offering a low-carbon solution for power generation and transportation. However, efficient storage and transport remain challenges due to hydrogen's low density, high diffusivity, and flammable nature, necessitating the development of practical hydrogen storage technologies. Among the various methods, $NaBH_4$ has emerged as a viable hydrogen storage material because of its stability and ability to release hydrogen gas upon hydrolysis [4-6]. The use of $NaBH_4$ for hydrogen storage offers several advantages. It allows for safe, compact, and efficient hydrogen storage and transport, addressing key challenges associated with conventional hydrogen storage. $NaBH_4$ is particularly advantageous due to its solid form, which simplifies handling and minimizes safety risks. Furthermore, it provides a high hydrogen content by weight, making it attractive for applications requiring high energy density [7-9]. The hydrolysis of $NaBH_4$ is a straightforward, low-cost process that generates hydrogen gas under mild conditions, ensuring high-purity hydrogen without the risk of contamination or undesirable side reactions [10, 11]. The effectiveness of $NaBH_4$ hydrolysis depends significantly on the catalysts used to promote the reaction. Transition metal oxides and other nanomaterials have been widely explored as catalysts for this purpose, aiming to enhance hydrogen production rates and reduce activation energy barriers [5, 7, 12]. Notable studies in the field include the work of Changwoo Kim et al. [13] who synthesized cobalt oxide nanorods (wz-CoO-NRs) via the thermal decomposition of cobalt oleate and cobalt stearate. Their study demonstrated that wz-CoO-NRs achieved a hydrogen production rate of 10,367 mL $min^{-1}$ $g^{-1}$ at 293 K with an activation energy of 27.4 kJ $mol^{-1}$, highlighting the importance of morphology and surface characteristics for catalytic efficiency. Similarly, Guo et al. [14], developed NiCoB hollow nanospheres using galvanic replacement. These nanospheres exhibited superior catalytic activity with a hydrogen production rate of 6400 mL $H_2$ $min^{-1}$ $g^{-1}$ at 303 K and an activation energy of 33.1 kJ $mol^{-1}$, attributed to their large surface area and electronic effects. In another study, Kılınç and Şahin [15], synthesized a Zn complex of *4,4'-methylenebis(2,6-diethyl)aniline-3,5-di-tert-butylsalicylaldimine* and characterized its catalytic performance for $NaBH_4$ hydrolysis. Their results indicated activation energy of 22.978 kJ $mol^{-1}$, with hydrogen generation rates of 952.5 mmol $H_2$ $g^{-1}$ $min^{-1}$ at 50°C and 614.4 mmol $H_2$ $g^{-1}$ $min^{-1}$ at 30°C, demonstrating the critical role of synthesis parameters in determining catalytic efficiency.

Given the growing demand for environmentally friendly hydrogen production, the exploration of green synthesis methods for catalysts has gained momentum. Green synthesis techniques, which employ environmentally benign solvents, plant extracts, and renewable precursors, offer a sustainable approach to catalyst development. In the study achieved by Boro et al., they investigated the green synthesis of ZnO nanoparticles using ethanolic leaf extract of Xanthium indicum, a plant native to North East India with pharmaceutical applications. The ZnO nanoparticles were characterized by DLS, TEM, FTIR, UV-Vis and XRD and showed high antioxidant, antimicrobial, antifungal and photocatalytic activities compared to their chemically synthesized counterparts. This eco-friendly approach offers a cost-effective alternative by reducing the need for toxic reagents and energy-intensive processes. The findings highlight the potential of green ZnO nanoparticles for applications in nanodevices, energy storage and healthcare [16]. Naiel et al. synthesized zinc oxide (ZnO) nanoparticles using the aqueous extract of Limonium pruinosum (sea lavender). The ZnO NPs exhibited an average size of ~41 nm and a hexagonal/cubic crystal structure. The findings highlight the biocompatibility, environmental friendliness, and cost-effectiveness of these ZnO NPs, making them promising candidates for biomedical and therapeutic applications [17]. ZnO is known for its high surface area, chemical stability, and catalytic versatility, making it suitable for various industrial applications, including hydrogen production [18, 19]. Furthermore, ZnO's non-toxic nature aligns with sustainability goals, ensuring safer handling and reduced environmental impact compared to other catalytic materials [20, 21]. In this context, zinc oxide (ZnO) synthesized via green chemistry principles presents an attractive candidate for $NaBH_4$ hydrolysis reactions.

This study aims to investigate the catalytic performance of green-synthesized ZnO in $NaBH_4$ hydrolysis reactions. By using a sustainable synthesis route, this research contributes to the development of eco-friendly catalysts while addressing key challenges in hydrogen storage and production. The findings are expected to advance the practical application of $NaBH_4$ as a hydrogen carrier and promote the integration of green chemistry principles in catalytic material design.

## 2. MATERIAL AND METHOD

The ZnO nanoparticles were synthesized through an environmentally friendly method using turmeric extract without any toxic reducing chemicals. To prepare the turmeric extract, 10 grams of turmeric powder were weighed and mixed with 100 mL of 70% ethanol. The mixture was shaken well for 5 minutes and then allowed

to soak for two days at room temperature (approximately 25-30°C). The resulting ethanol extract was filtered using qualitative Whatman filter paper no.1 (125 mm) and stored at 4°C. For the synthesis of ZnO nanoparticles, a zinc (II) nitrate solution at a concentration of 10 mM was combined with 50 mL of the turmeric ethanolic extract and incubated at 60°C for 60 minutes in a dark room. Afterward, the mixture was cooled to 25°C for 24 hours, followed by centrifugation at 3600 rpm for 30 minutes. The product was then washed several times with distilled water and ethanol. Finally, a dark brown precipitate was formed, which was dried at 90°C for 1 hour. The synthesized ZnO nanoparticles (NPs) were analyzed using various techniques. Scanning electron microscopy (SEM) was performed on a JEOL JSM-5500LV. Energy dispersive X-ray analysis (EDX) was conducted with an X-ray micro-analyzer (Oxford *6587,* INCA) attached to the SEM, operating at 20 kV. Transmission electron microscopy (TEM) was carried out on a Thermo Scientific Talos F200i using carbon-coated grids (Type G 200, 3.05 µm diameter). The zeta potential of the NPs was measured using a Malvern Panalytical instrument with ethanol as the dispersant. UV-Visible absorption spectroscopy was performed using a Unicam UV-VIS spectrophotometer UV2. To determine the rate of hydrogen generation, a hydrolysis reaction was conducted using a continuous system. Initially, 0.15 g of $NaBH_4$ was added to the reaction vessel in the absence of a catalyst, and the volume of hydrogen gas produced was measured over a period of 900 seconds. Subsequently, the experiment was repeated under the same conditions with the addition of 0.15 g of ZnO catalyst to the reaction mixture. Both were introduced into a two-neck flask, and the resulting hydrogen gas was captured and measured using an inverted, solution-immersed graduated cylinder. The volume of hydrogen gas collected in the graduated cylinder was carefully recorded, and adjustments were made to account for the volume changes due to the evaporation of water at the reaction temperature. This method ensured accurate measurement of the hydrogen gas produced, allowing for a precise determination of the catalytic activity of ZnO in the hydrolysis reaction of $NaBH_4$. The presence of ZnO catalyst enhanced the hydrogen generation rate, which was systematically compared to the control reaction without the catalyst.

## 3. RESULTS

In this study, we aimed to synthesize ZnO nanoparticles through an environmentally friendly method using ethanolic extract of turmeric. Turmeric is a commonly used spice in India and other Asian countries. The main active ingredient in turmeric is curcumin, chemically known as "*(1E,6E)-1,7-bis(4-hydroxy-3-methoxyphenyl)hepta-1,6-diene-3,5-dione*" (Figure 1).

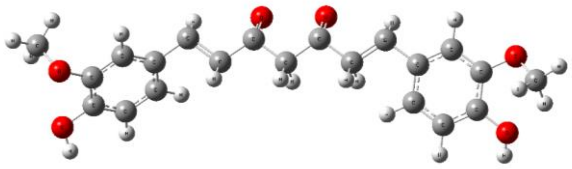

**Figure 1.** The molecular structure of curcumin

As illustrated in Figure 1, curcumin features two hydroxy groups (-OH) and two methoxy groups ($-OCH_3$) on its aromatic phenyl rings. These rings are connected by a heptadiene chain with two conjugated double bonds (C=C), creating a rigid and planar structure [22, 23]. Curcumin appears as a yellow to orange solid, with limited solubility in water but good solubility in organic solvents such as ethanol, methanol, and acetone. Its phenolic groups contribute to its well-documented antioxidant and anti-inflammatory properties [24-26].

The synthesized ZnO NPs were analyzed by SEM-EDX and related results were given in Figure 2. SEM-EDX analysis is a very useful method for morphological and compositional data for analyzing NPs. The granular shaped ZnO NPs were detected in SEM image with 0.791 µm average diameter. The precision with which the elemental composition of ZnO may be obtained makes these methods very useful for their analysis. The ZnO NPs EDX spectrum was shown in Figure 2, where zinc (Zn) and oxygen (O) are represented by separate peaks. The successful production of zinc oxide is confirmed by the presence of these Zn and O peaks in the EDX spectrum. The weight% values of Zn and O were 57 and 43%, respectively.



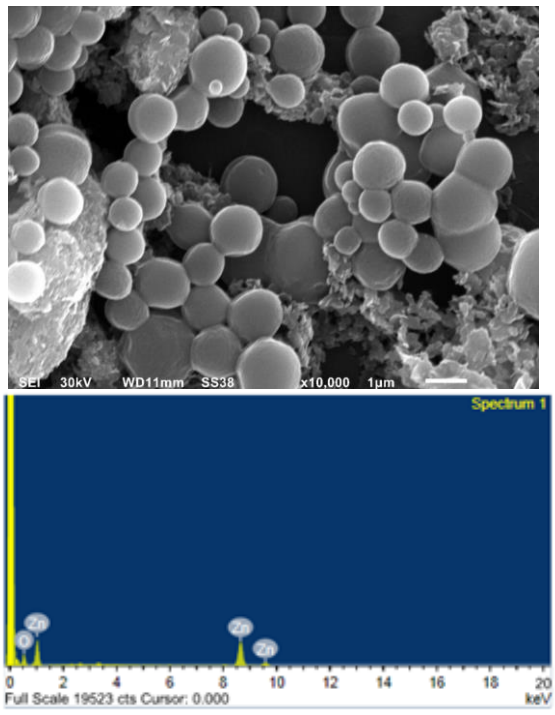


**Figure 2.** SEM-EDX anaysis of ZnO

Sadiya Samar et al. [27] synthesized ZnO via extract of Chenopodium album leaf, agglomeration was detected as the similar situation in Figure 2. Production of ZnO using green synthetic route was achieved by Boro et al.

[16] via ethanolic leaf extract of Xanthium indicum plant which is available only in North-East India. According to morphological analysis results, same structural view was detected.

TEM study was carried out after SEM-EDX investigation to obtain a more complete understanding of the ZnO structure. While the following TEM examination revealed higher resolution imaging and deeper insights into the crystalline structure of the ZnO samples, the SEM-EDX initially provided surface morphology and elemental composition data.

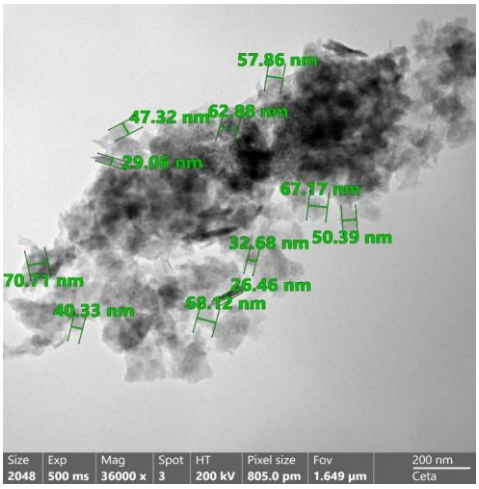


**Figure 3.** TEM anaysis of ZnO

As seen from Figure 3, the partice size was ranged between 30 nm and 70 nm. The distribution of sizes at the nanoscale is highly useful for catalytic processes, like the hydrolysis of $NaBH_4$. Because smaller particles have a larger surface area to volume ratio, there are more active sites available for catalytic reactions. The efficiency and rate of the hydrolysis process can be greatly enhanced by this greater surface area, resulting in more efficient production of hydrogen. Catalytic performance can be achieved by exact control over particle size and distribution, as demonstrated by TEM investigation. These characteristics together demonstrate ZnO nanoparticles' potential as an efficient catalyst in a range of chemical reactions, including the efficient and sustainable hydrolysis of $NaBH_4$ to produce hydrogen. According to literature the synhesis mechanism can be clarifed, for this purpose UV analysis should be helpful. The obtained results were given in Figure 4.

Curcumin is a beta-diketone characterized by the replacement of two hydrogen atoms with feruloyl groups, existing in two tautomeric forms: keto and enol [28, 29]. The keto form predominates in acidic and neutral pH environments, while the enol form is stable in alkaline conditions. Structurally, curcumin comprises a seven-carbon linker and three key functional groups: an α, β-unsaturated β-diketone moiety, an aromatic O-methoxy-phenolic group, and a seven-carbon chain. The α, β-unsaturated carbonyl groups bridge the aromatic rings, and the diketones can deprotonate to form enolates, with the α, β-unsaturated carbonyl acting as a acceptor for nucleophilic addition. The antioxidant properties of curcumin are due to its phenolic groups, while its hydrophobic character stems from the carbon linker. To enhance its biological activity, curcumin has been modified, taking advantage of its strong metal-chelating properties via the α, β-unsaturated β-diketo moiety [30, 31].

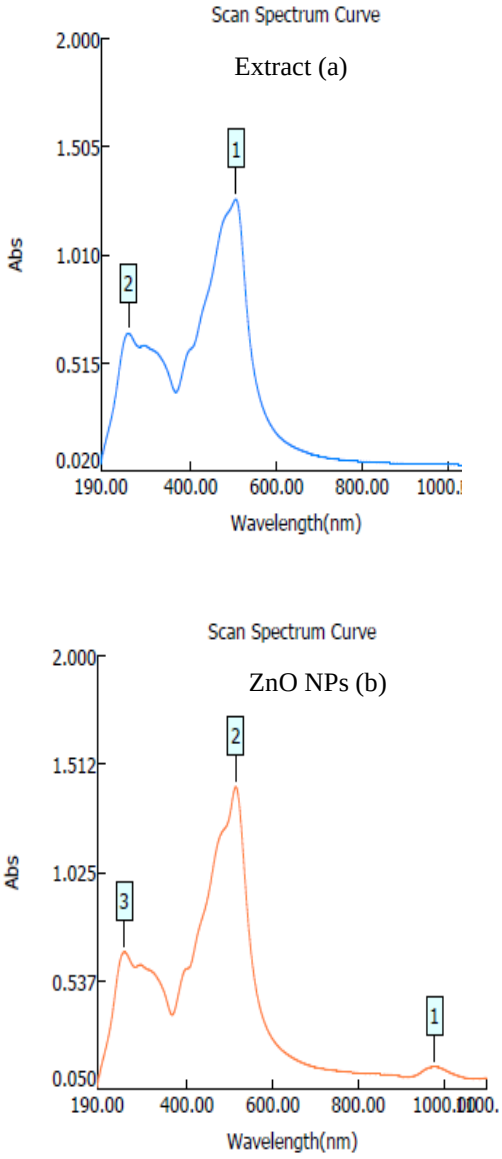


**Figure 4.** The UV sprectra of extract (a) and ZnO (b)

UV-vis spectroscopy was employed to study metal binding to curcumin, which typically occurs through the β-diketone group via chelation. This process involves the formation of dative covalent bonds, where one atom provides both electrons for the bond, introducing semipolar characteristics [32]. Metal coordination often involves one or two curcumin molecules, occasionally three, as seen in some complexes like the hexagonal structure. Metal-curcumin binding through the enolic group induces structural changes, with variations in metal-oxygen bond lengths and coordination geometries depending on the metal-to-curcumin ratio [32]. ZnO exhibited absorption peaks in its UV spectra at 253 nm, 513 nm, and 977 nm. The ZnO material's structural features and several electronic transitions are responsible for these peaks. The intrinsic bandgap absorption of

ZnO, which correlated to the electrical transition from the valence band to the conduction band, was most likely the cause of the absorption peak at 253 nm. This peak is associated with the excitonic absorption typical of ZnO nanostructures, and ZnO has a wide bandgap of about 3.37 eV. The ZnO lattice's defect states or impurities could be related to the peak at 513 nm. Defect states like oxygen vacancies or zinc interstitials can produce additional absorption features in the visible spectrum by generating localized energy levels within the bandgap. Surface states or deep-level imperfections may be the cause of the absorption peak at 977 nm. These deep-level flaws have the ability to trap electrons and aid in near-infrared absorption. Surface states or plasmonic phenomena resulting from ZnO's contact with its surroundings may possibly play a role in this absorption property [33-35]

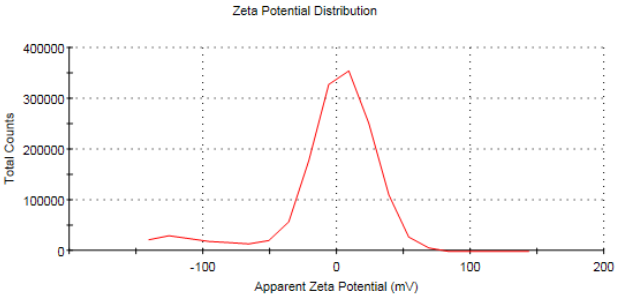


**Figure 5.** The zeta potential of ZnO

Figure 5 showed the zeta potential measurements for ZnO nanoparticles (NPs). Typically, ZnO NPs with a size of approximately 5 nm exhibit zeta potential values ranging from -20 mV to +20 mV Ateş [36] Generally, ZnO NPs possessing a zeta potential less than -10 mV demonstrate increased stability in aqueous solutions due to electrostatic repulsion, which prevents particle aggregation. In the current study, the measured zeta potential value was -5.78 mV. According to the literature, zeta potential values closer to zero indicate a propensity for particle agglomeration due to reduced electrostatic repulsion. Zeta potential is a critical parameter in evaluating the colloidal stability of nanoparticle suspensions. Higher absolute values of zeta potential (either positive or negative) suggest stronger repulsive forces between particles, thereby enhancing stability [37]. Conversely, lower absolute values, as observed here, suggest weaker repulsive interactions and a higher likelihood of aggregation. The measured zeta potential of -5.78 mV for ZnO NPs indicates that while there is some repulsion, it is insufficient to prevent agglomeration entirely [38]. Thus, the ZnO NPs in this study were prone to agglomeration (as seen in SEM micropgraph)

The catalytic behavior of ZnO was investigated and related results were presented in Figure 6.

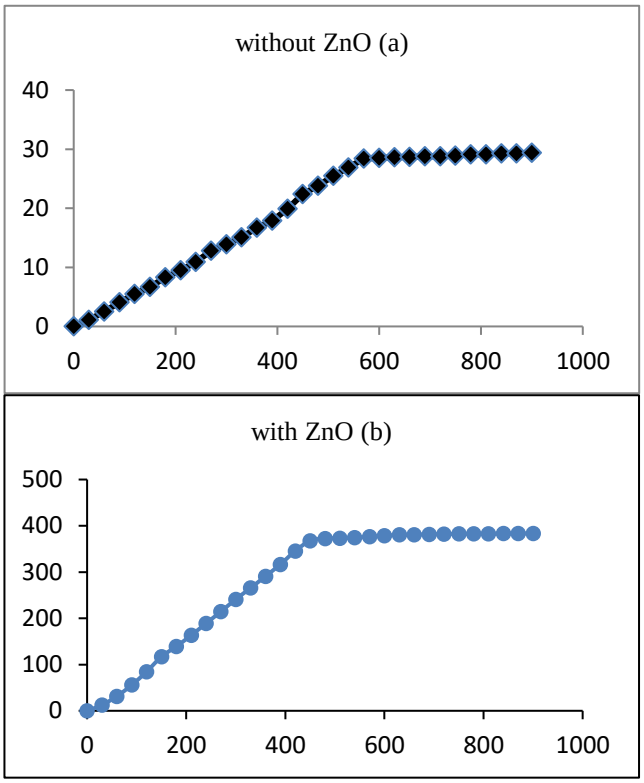


**Figure 6.** The hydrogen gas volume in the absence (a) and presence (b) of ZnO NPs catalyst

According to obtained result the produced hydrogen gas was 29.4 mL after 560 s, in the absence of ZnO but the value was increased almost 13 times in presence of ZnO NPs. The obtained hdrogen gas was almost 383.4 mL in the presence of ZnO after 430 s.



**Table 1.** Comparative analysis of catalysts for hydrogen generation from $NaBH_4$ under various conditions

| Catalysts | Size (nm) | Catalyst (mg) | Conditions | HGR ($mLH_2\ g^{-1}\ min^{-1}$) | References |
|---|---|---|---|---|---|
| Ni-B | - | Foam | 20 wt% $NaBH_4$, 5 wt% NaOH, 60 $^0C$ | 130 | [39] |
| $CuFe_2O_4$/RGO | 5 | 30 | 40 mg $NaBH_4$ | 622 | [40] |
| Ni | - | 75 wt% | 14 wt% $NaBH_4$, 30 $^0C$ | 96.3 | [41] |
| Ni-Ru/50WX8 | 20-60 | 200 | 10 wt% $NaBH_4$, 5 wt% NaOH, 35 $^0C$ | 400 | [42] |
| G-CoB | 15-100 | 100 | 568 mg $NaBH_4$, 20 $^0C$ | 258 | [43] |
| Ru-Ni/Ni | - | - | 20 wt% $NaBH_4$, 1 wt% NaOH, 30 $^0C$ | 360 | [44] |
| $Pt/Co_3O_4$ | 39.8 | 10 | 100 mg $NaBH_4$ | 120 | [45] |
| ZnO NPs | 30-70 | 150 | 150 mg $NaBH_4$, 25 $^0C$ | 356.5 | In this study |

A comparative analysis of catalysts for producing hydrogen from $NaBH_4$ under various circumstances was shown in Table 1, using 150 mg of $NaBH_4$ at 25°C, our work showed hydrogen generation rate (HGR) of 356.5 $mLH_2\ g^{-1}\ min^{-1}$ using ZnO nanoparticles (NPs) with a size range of 30–70 nm. Because of this performance, ZnO NPs can compete with other catalysts. $CuFe_2O_4$/RGO, for example, demands a greater $NaBH_4$ load (40 mg) and smaller particle sizes (5 nm), although achieving a HGR of 622 $mLH_2\ g^{-1}\ min^{-1}$. This suggests that material synthesis needs to be tightly controlled. In this study, ZnO NPs perform better than some catalysts

that use more material and complex compositions. For instance, Ni-B foam achieves 130 $mLH_2$ $g^{-1}$ $min^{-1}$ at 60°C, whereas $Pt/Co_3O_4$ only reaches 120 $mLH_2$ $g^{-1}$ $min^{-1}$ with 10 mg of catalyst. Additionally, Ni-Ru/50WX8 shows a higher HGR of 400 $mLH_2$ $g^{-1}$ $min^{-1}$ but requires 200 mg of catalyst and operates at 35°C, demonstrating that ZnO NPs offer a simpler, scalable option under this condition. ZnO NPs are effective and useful catalyst that offers a high rate of hydrogen generation under comparatively simple circumstances. Higher HGRs are produced by some catalysts, although they frequently require greater amounts of material, intricate compositions, or higher temperatures. This study showcases the scalability and simplicity of ZnO NPs for sustainable hydrogen generation, with opportunities for future work focused on optimizing reagent concentrations and exploring synergistic catalyst combinations.

## 4. DISCUSSION AND CONCLUSION

The synthesized ZnO NPs demonstrated high potential for catalytic applications, particularly in the hydrolysis of $NaBH_4$ for hydrogen generation. SEM-EDX analysis confirmed the granular morphology of the ZnO NPs with an average diameter of 0.6 µm and provided precise compositional data, indicating a Zn to O weight ratio of 57% to 43%. The particle size distribution ranged from 30 nm to 70 nm, enhancing catalytic efficiency due to the increased surface area-to-volume ratio, which provides more active sites for reactions. UV spectroscopy revealed absorption peaks at 253 nm, 513 nm, and 977 nm, attributed to intrinsic bandgap absorption, defect states, and surface states, respectively. The zeta potential measurement of -5.78 mV indicated moderate stability in aqueous solutions, although some agglomeration was seen. Despite this, the ZnO NPs significantly improved hydrogen production in the $NaBH_4$ hydrolysis reaction, increasing the volume of hydrogen generated from 29.4 mL to 383.4 mL, demonstrating a nearly 13-fold enhancement. These findings highlight the importance of particle size control and surface characteristics in optimizing the catalytic performance of ZnO NPs, making them a promising material for efficient hydrogen generation.

## Acknowledgement

We are greatly thankful to Khaled M. Elattar for his valuable guidance.

## Conflict of Interest

There are no conflicts of interest declared by any of the writers.

## REFERENCES

[1] Şahin Ö, Baytar O, Kutluay S, Ekinci A. Potential of nickel oxide catalyst from banana peel extract via green synthesis method in both photocatalytic reduction of methylene blue and generation of hydrogen from sodium borohydride hydrolysis. Journal of Photochemistry and Photobiology A: Chemistry. 2024;448:115301.

[2] Onat E. Synthesis of a cobalt catalyst supported by graphene oxide modified perlite and its application on the hydrolysis of sodium borohydride. Synthetic Metals. 2024;306:117621.

[3] Li Q, Wang F, Zhou X, Chen J, Tang C, Zhang L. Synergistical photo-thermal-catalysis of Zn2GeO4:xFe3+ for H2 evolution in NaBH4 hydrolysis reaction. Catalysis communications. 2021;156:106321.

[4] Abdelhamid HN. A review on hydrogen generation from the hydrolysis of sodium borohydride. International Journal of Hydrogen Energy. 2021;46(1):726-65.

[5] Prasad D, Patil KN, Sandhya N, Chaitra CR, Bhanushali JT, Samal AK, et al. Highly efficient hydrogen production by hydrolysis of NaBH4 using eminently competent recyclable Fe2O3 decorated oxidized MWCNTs robust catalyst. Applied Surface Science. 2019;489:538-51.

[6] Zou Y, Yin Y, Gao Y, Xiang C, Chu H, Qiu S, et al. Chitosan-mediated Co–Ce–B nanoparticles for catalyzing the hydrolysis of sodium borohydride. International Journal of Hydrogen Energy. 2018;43(10):4912-21.

[7] Kılınç D, Şahin Ö. Effective TiO2 supported Cu-Complex catalyst in NaBH4 hydrolysis reaction to hydrogen generation. International Journal of Hydrogen Energy. 2019;44(34):18858-65.

[8] Wei Y, Meng W, Wang Y, Gao Y, Qi K, Zhang K. Fast hydrogen generation from NaBH4 hydrolysis catalyzed by nanostructured Co–Ni–B catalysts. International Journal of Hydrogen Energy. 2017;42(9):6072-9.

[9] Wang L, Li Z, Zhang Y, Zhang T, Xie G. Hydrogen generation from alkaline NaBH4 solution using electroless-deposited Co–Ni–W–P/γ-Al2O3 as catalysts. Journal of Alloys and Compounds. 2017;702:649-58.

[10] Lin K-YA, Chang H-A. Efficient hydrogen production from NaBH4 hydrolysis catalyzed by a magnetic cobalt/carbon composite derived from a zeolitic imidazolate framework. Chemical Engineering Journal. 2016;296:243-51.

[11] Chou C-C, Hsieh C-H, Chen B-H. Hydrogen generation from catalytic hydrolysis of sodium borohydride using bimetallic Ni–Co nanoparticles on reduced graphene oxide as catalysts. Energy. 2015;90:1973-82.

[12] Aman D, Alkahlawy AA, Zaki T. Hydrolysis of NaBH4 using ZVI/Fe2(MoO4)3 nanocatalyst. International Journal of Hydrogen Energy. 2018;43(39):18289-95.

[13] Kim C, Lee SS, Li W, Fortner JD. Towards optimizing cobalt based metal oxide nanocrystals

for hydrogen generation via NaBH4 hydrolysis. Applied Catalysis A: General. 2020;589:117303.
[14] Guo J, Hou Y, Li B, Liu Y. Novel Ni–Co–B hollow nanospheres promote hydrogen generation from the hydrolysis of sodium borohydride. International Journal of Hydrogen Energy. 2018;43(32):15245-54.
[15] Kılınç D, Şahin Ö. Performance of Zn-Schiff Base complex catalyst in NaBH4 hydrolysis reaction. International Journal of Hydrogen Energy. 2020;45(60):34783-92.
[16] Boro B, Boruah JS, Devi C, Alemtoshi, Gogoi B, Bharali P, et al. A novel route to fabricate ZnO nanoparticles using Xanthium indicum ethanolic leaf extract: Green nanosynthesis perspective towards photocatalytic and biological applications. Journal of Molecular Structure. 2024;1300:137227.
[17] Naiel B, Fawzy M, Halmy MWA, Mahmoud AED. Green synthesis of zinc oxide nanoparticles using Sea Lavender (Limonium pruinosum L. Chaz.) extract: characterization, evaluation of anti-skin cancer, antimicrobial and antioxidant potentials. Scientific Reports. 2022;12(1):20370.
[18] Goswami S, Bishnoi A, Tank D, Patel P, Chahar M, Khaturia S, Modi N, Khalid M, Alam MW, Kumar Yadav V, Alreshidi MA, Yadav KK. Recent trends in the synthesis, characterization and commercial applications of zinc oxide nanoparticles- a review. Inorganica Chimica Acta. 2024;573:122350.
[19] Bakranova D, Nagel D. ZnO for Photoelectrochemical Hydrogen Generation. Clean Technologies. 2023;5(4):1248-68.
[20] Gadewar M, Prashanth GK, Ravindra Babu M, Dileep MS, Prashanth PA, Rao S, Mahadevaswamy M, Kumar Ghosh M, Singh N, Mandotra SK, Chauhan A, Rustagi S, Yogi R, Chinnam S, Ali B, Ercisli S, Orhan E. Unlocking nature's potential: Green synthesis of ZnO nanoparticles and their multifaceted applications – A concise overview. Journal of Saudi Chemical Society. 2024;28(1):101774.
[21] Zhou X-Q, Hayat Z, Zhang D-D, Li M-Y, Hu S, Wu Q, Cao Y-F, Yuan Y. Zinc Oxide Nanoparticles: Synthesis, Characterization, Modification, and Applications in Food and Agriculture. Processes. 2023;11(4):1193.
[22] Zhai K, Brockmüller A, Kubatka P, Shakibaei M, Büsselberg D. Curcumin's Beneficial Effects on Neuroblastoma: Mechanisms, Challenges, and Potential Solutions. Biomolecules. 2020;10(11):1469.
[23] Badmanaban R, Dhananjoy S, Dhrubo JS, Arpita B, Supradip M, Susmita B. Turmeric: A holistic Solution for Biochemical malfunction. Research Journal of Pharmacy and Technology. 2021; 14(10):5540-0.
[24] Hani U, Shivakumar HG. Solubility enhancement and delivery systems of curcumin a herbal medicine: a review. Current Drug Delivery. 2014;11(6):792-804.
[25] Ipar VS, Dsouza A, Devarajan PV. Enhancing Curcumin Oral Bioavailability Through Nanoformulations. European Journal of Drug Metabolism and Pharmacokinetics. 2019;44(4):459-80.
[26] Sharifi-Rad J, Rayess YE, Rizk AA, Sadaka C, Zgheib R, Zam W, Sestito S, Rapposelli S, Neffe-Skocińska K, Zielińska D, Salehi B, Setzer WN, Dosoky NS, Taheri Y, El Beyrouthy M, Martorell M, Ostrander EA, Suleria HAR, Cho WC, Maroyi A, Martins N. Turmeric and Its Major Compound Curcumin on Health: Bioactive Effects and Safety Profiles for Food, Pharmaceutical, Biotechnological and Medicinal Applications. Frontiers in Pharmacology. 2020;11:01021.
[27] Samar S, Kumar A, Kumar P. Green synthesis of ZnO nano-crystals using Chenopodium album L. Leaf extract, their characterizations and antibacterial activities. Materials Science and Engineering: B. 2024;299:117005.
[28] Lee WH, Loo CY, Bebawy M, Luk F, Mason RS, Rohanizadeh R. Curcumin and its derivatives: their application in neuropharmacology and neuroscience in the 21st century. Current Neuropharmacology. 2013;11(4):338-78.
[29] Cornago P, Claramunt RM, Bouissane L, Alkorta I, Elguero J. A study of the tautomerism of β-dicarbonyl compounds with special emphasis on curcuminoids. Tetrahedron. 2008;64(35):8089-94.
[30] Ciuca MD, Racovita RC. Curcumin: Overview of Extraction Methods, Health Benefits, and Encapsulation and Delivery Using Microemulsions and Nanoemulsions. International Journal of Molecular Sciences. 2023;24(10).
[31] Kawano S-i, Inohana Y, Hashi Y, Lin J-M. Analysis of keto-enol tautomers of curcumin by liquid chromatography/mass spectrometry. Chinese Chemical Letters. 2013;24(8):685-7.
[32] Prasad S, DuBourdieu D, Srivastava A, Kumar P, Lall R. Metal-Curcumin Complexes in Therapeutics: An Approach to Enhance Pharmacological Effects of Curcumin. International Journal of Molecular Sciences. 2021;22(13):7094.
[33] Song Z, Timothy A. Kelf, Washington H. Sanchez, Michael S. Roberts, Jaro Rička, Martin Frenz, et al. Characterization of optical properties of ZnO nanoparticles for quantitative imaging of transdermal transport. Biomedical Optics Express. 2011;2(12):3321-33.
[34] Singh S, Gade JV, Verma DK, Elyor B, Jain B. Exploring ZnO nanoparticles: UV–visible analysis and different size estimation methods. Optical Materials. 2024;152:115422.
[35] Singh DK, Pandey DK, Yadav RR, Singh D. A study of nanosized zinc oxide and its nanofluid. Prama. 2012;78(5):759-66.
[36] Ateş M. Nanoparçacıkların Ölçme ve İnceleme Teknikleri. Turkish Journal of Scientific Reviews. 2018;11(1):63-9.
[37] Marsalek R. Particle Size and Zeta Potential of ZnO. APCBEE Procedia. 2014;9:13-7.
[38] Günay K, Leblebici Z, Koca FD. Çinko Nanopartiküllerinin (ZnO NP) Biyosentezi, Karakterizasyonu ve Anti- Bakteriyel Etkisinin İncelenmesi. Nevşehir Bilim Teknoloji Dergisi. 2021;10(1):56-66.

[39] Lee JK, Ann H-h, Yi Y, Lee KW, Uhm S, Lee J. A stable Ni–B catalyst in hydrogen generation via NaBH4 hydrolysis. Catalysis Communications. 2011;16(1):120-3.
[40] Tang M, Xia F, Gao C, Qiu H. Preparation of magnetically recyclable CuFe2O4/RGO for catalytic hydrolysis of sodium borohydride. International Journal of Hydrogen Energy. 2016;41(30):13058-68.
[41] Kim J-H, Kim K-T, Kang Y-M, Kim H-S, Song M-S, Lee Y-J, Lee PS, Lee J-Y. Study on degradation of filamentary Ni catalyst on hydrolysis of sodium borohydride. Journal of Alloys and Compounds. 2004;379(1):222-7.
[42] Liu C-H, Chen B-H, Hsueh C-L, Ku J-R, Jeng M-S, Tsau F. Hydrogen generation from hydrolysis of sodium borohydride using Ni–Ru nanocomposite as catalysts. International Journal of Hydrogen Energy. 2009;34(5):2153-63.
[43] Zhang F, Hou C, Zhang Q, Wang H, Li Y. Graphene sheets/cobalt nanocomposites as low-cost/high-performance catalysts for hydrogen generation. Materials Chemistry and Physics. 2012;135(2):826-31.
[44] Wang F, Luo Y, Wang Y, Zhu H. The preparation and performance of a novel spherical spider web-like structure RuNi / Ni foam catalyst for NaBH4 methanolysis. International Journal of Hydrogen Energy. 2019;44(26):13185-94.
[45] Hung T-F, Kuo H-C, Tsai C-W, Chen HM, Liu R-S, Weng B-J, Lee J-F. An alternative cobalt oxide-supported platinum catalyst for efficient hydrolysis of sodium borohydride. Journal of Materials Chemistry. 2011;21(32):11754-9.